# HIGHEST SURGE IN THE NORTH SEA

by

S. Ishiguro

Report No. 36

1976

NATURAL ENVIRONMENT RESEARCH COUNCIL
INSTITUTE OF OCEANOGRAPHIC SCIENCES

**INSTITUTE OF OCEANOGRAPHIC SCIENCES**

Wormley, Godalming,
Surrey, GU8 5UB.
(0428 - 79 - 4141)

(Director: Professor H. Charnock)

Bidston Observatory,
Birkenhead,
Merseyside, L43 7RA.
(051-653-8633)
(Assistant Director: Dr. D. E. Cartwright)

Crossway,
Taunton,
Somerset, TA1 2DW.
(0823-86211)
(Assistant Director: M.J. Tucker)

Marine Scientific Equipment Service
Research Vessel Base,
No. 1 Dock,
Barry,
South Glamorgan, CF6 6UZ.
(04462-77451)
(Officer-in-Charge: Dr. L.M. Skinner)

---

*On citing this report in a bibliography the reference should be followed by the words UNPUBLISHED MANUSCRIPT.*

# HIGHEST SURGE IN THE NORTH SEA

S. ISHIGURO

REPORT NO. 36

1976

Institute of Oceanographic Sciences,
Brook Road,
Wormley, Godalming, Surrey GU8 5UB

Contents


31 pages with 26 diagrams and 5 tables

This work has been carried out in a limited period of time to meet a specific requirement. This report has been re-arranged for general readers.

Abstract A method of estimating the highest storm surge at an arbitrary position in the North Sea is described. A set of hydrodynamic equations has been solved, by an electronic model, for an instantaneously applied uniform wind field (constant speed) over the sea, and for an instantaneously applied uniform pressure field (constant gradient) again over the sea, each having two rectangular directions, i. e. four cases in all. The regional variations of response time of the sea surface to the four cases have also been computed. Each of these response times is combined with the reduction factor by which an estimated hourly-mean wind speed can be converted into the speed for an arbitrary averaging period, by assuming that the surge height at each position in the sea becomes maximum when the averaging period is equal to the response time. The results are summarised in four diagrams from which four parameters can be obtained for an arbitrary position in the sea under a given hourly-mean wind speed, so that the highest surge at this position can be obtained as a vector sum, with additional simple calculations. As an example, a diagram for estimating the highest surges for the whole area of the North Sea, under a certain wind speed (a proposed extreme wind speed for the average recurrence period of 50 years), together with wind directions, are shown with comparisons with some special cases and a similar result obtained by another method; and all the results are explained physically.

## 1. Introduction

The estimation of the highest surge in the North Sea, in conjunction with its wind-generated waves and tides etc., has often been required for coastal or offshore structures. Such a surge height depends on estimated extreme meteorological conditions which are related to a position in the sea and a recurrence period considered, as well as hydrodynamic relationships between the air and water in the sea.

The estimation of the highest surge is, therefore, often required for a different position in the sea and different meteorological conditions. In order to meet these requirements, a set of diagrams by which the highest surges at an arbitrary position in the North Sea under a given wind speed and duration can be estimated have been made (Ishiguro, 1966). This set has been used for answering individual inquiries (made to the IOS) on this problem, and for 'Guidance on the design and construction of offshore installations' (Department of Energy, 1974).

The above mentioned method offers a greater simplicity of use (an estimation can be made in a minute), but some assumptions have to be accepted. Improvements of the method are considered, in this paper, so that a large part of its assumptions can be removed, without sacrificing too much of its simplicity of use. (The newly built model is expected to remove most of the remaining assumptions).

## 2. An outline of the original method

Since the original paper (Ishiguro, 1966), on which this paper has been based, was in a limited edition, it is outlined here.

A set of the equations of motion and continuity, including terms for the effect of the earth's rotation etc., which is representing the hydrodynamic system of the North Sea, has been solved by using the depth-mean single-layer two-dimensional electronic model. The mixed grid sizes of 50km and 100km have been used, with no time increments (due to this particular technique). The model boundaries to other seas (or an open sea) are taken on the line between the Orkney Islands and Bergen (the northern boundary), and on the line between Margate and Calais (the southern boundary). These boundaries are terminated with conditions such that no reflections of long waves occur. The bottom friction is linearised with the coefficient of 0.24 cm/s.

A uniform and constant wind field is instantaneously applied to the whole sea surface of the modelled area, in the northern direction (along the long axis of the sea; 338° referred to geographical north, at the centre of the sea), and in the easterly direction (68°). The square-law relationship between the wind speed and water-surface stress, with the coefficient of $2.5 \times 10^{-3}$, has been applied.

A set of data representing the change of water surface height with time (continuous) at each grid, and a series of water-surface contour maps (hourly intervals) for 40h, both in the northerly and easterly components, have been obtained.

By taking the northerly and easterly components of water height on a particular grid and at a particular time (say 5, 10 or 30h), the maximum surge height is computed as a vector quantity; i.e. in the terms of the water height (referred to an undisturbed surface) and the direction of wind by which such a height is generated.

Some examples of the result are shown in Ref. 2. The procedure of using this set of diagrams is as follows:

(1) choose an appropriate set of height and direction diagrams, according to a given wind duration,

(2) choose a particular position in the sea for which an estimation of the highest surge is required,

(3) read the value of water height on that position on the diagram, and multiply the factor of $(S/20)^2$ to this value for obtaining the highest surge, where S is the wind speed in m/s, and

(4) read the value at the corresponding position on the direction diagram, for obtaining the wind direction.

In this procedure, (3) is the only calculation required. Even all the contours can be converted to a given wind speed, simply by multiplying this factor.

Although a simplicity in use is a great advantage of this method, some errors due to the omission of a pressure field (which always associates with a wind field) and the use of constant values for wind speed and duration (which is a very approximate representation of meteorological conditions) have to be accepted.

## 3. Improved method

An improved method, based on the method outlined in chapter 2, by which the highest surge in the North Sea can be estimated is described here.

The main differences of the improved method, compared with the original one, are as follows:

(a) A pressure field, which is omitted in the original method for simplicity of use, is now taken into account. (Note that a single diagram representing both wind and pressure fields cannot easily be generalised for an arbitrary wind speed, since their effects on a surge are not linearly related).

(b) The estimation of duration of wind, which is necessary for the original method, is no longer required.

(c) The regional variations of response time of the sea, which are not separately treated in the original method, are introduced so that these are combined with the duration of wind and pressure fields automatically.

(d) A set of four diagrams is used for estimating the highest surge for an arbitrary wind speed in the improved method, and about 10 minutes are required to obtain the result for an arbitrary position in the sea, with a conventional electronic pocket calculator with memory, instead of only one minute by the original method.

The procedure of making the method is as follows:

(1) A set of hydrodynamic equations, representing the North Sea on which a uniform wind field (constant speed) is applied instantaneously, and in two rectangular directions separately, has been solved first. See Appendix 1 for the indication of directions throughout this paper.

The results have been shown in Figs. 9, 10, 11 and 12 of Ref. 2. The height of wind-generated surges in these results are for the wind speed of 20 m/s, and the wind-stress coefficient of 2.5 x $10^{-3}$. From these data, a set of diagrams for estimating the height of wind-generated surge for an arbitrary wind speed has been made, by converting the unit used in the original diagrams into the unit of (surge height) / (wind speed)$^2$, as shown in Fig 1 (in this paper). Let us call them the $\zeta_{wx} / u_x^2$ and $\zeta_{wy}/u_y^2$ diagrams.

(2) From the same set of hydrodynamic equations, the regional variations of response time (a period between the start of application of a wind or pressure field and time when the surge height reaches 90% of its equilibrium value, or a peak value, if there is any peak before the equilibrium value) of the sea have been computed, in both rectangular directions.

The results have been shown in Fig. 54 of Ref. 4. Let us call them the $\tau_{wx}$ and $\tau_{wy}$ diagrams.

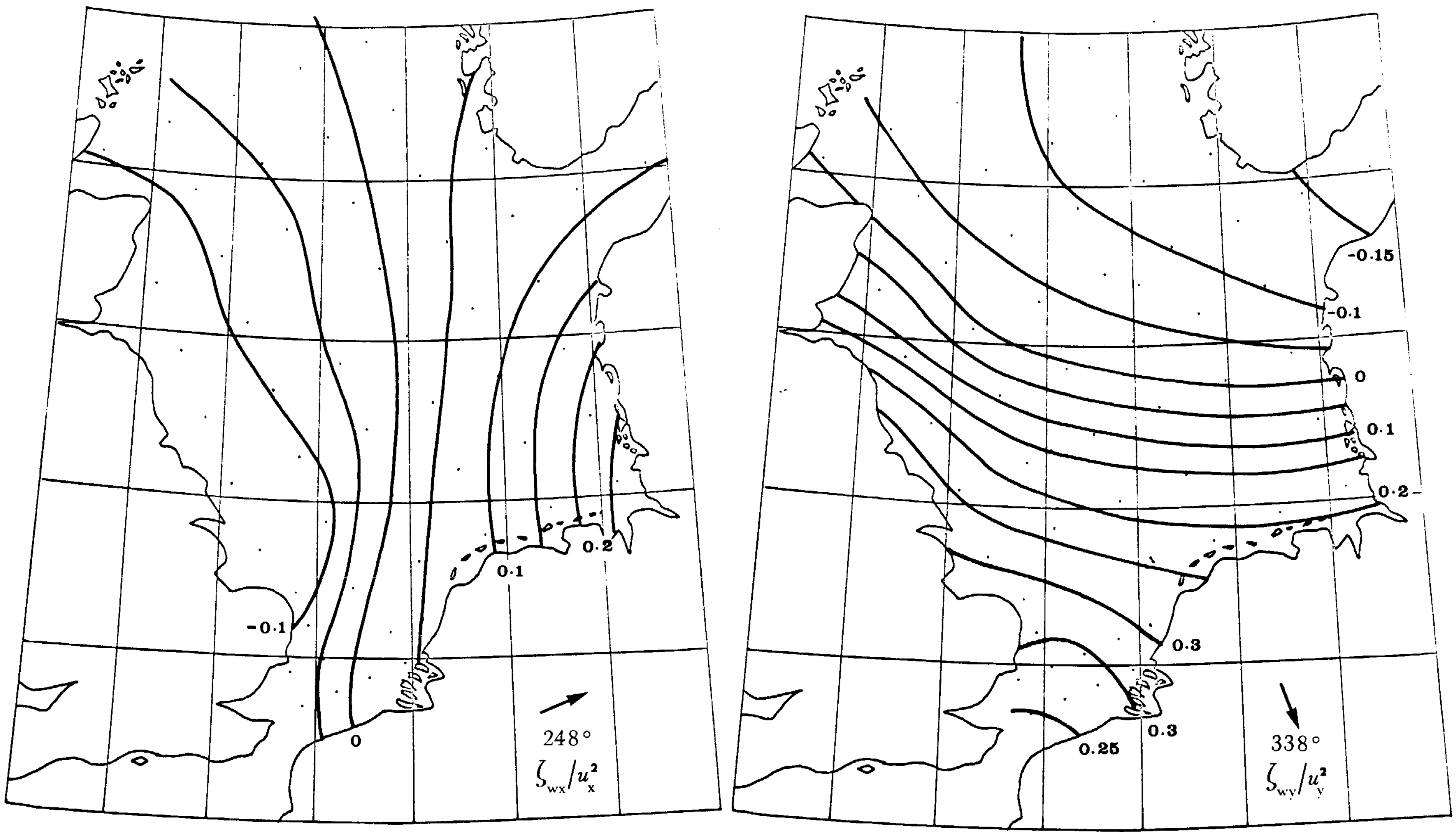


Fig. 1 Diagrams for estimating the equilibrium value of a surge height, $\zeta_x$ or $\zeta_y$ ( m), generated by a uniform wind field whose speed is $u_x$ or $u_y$ (m/s) respectively. Line value is in m/(m/s)$^2$.

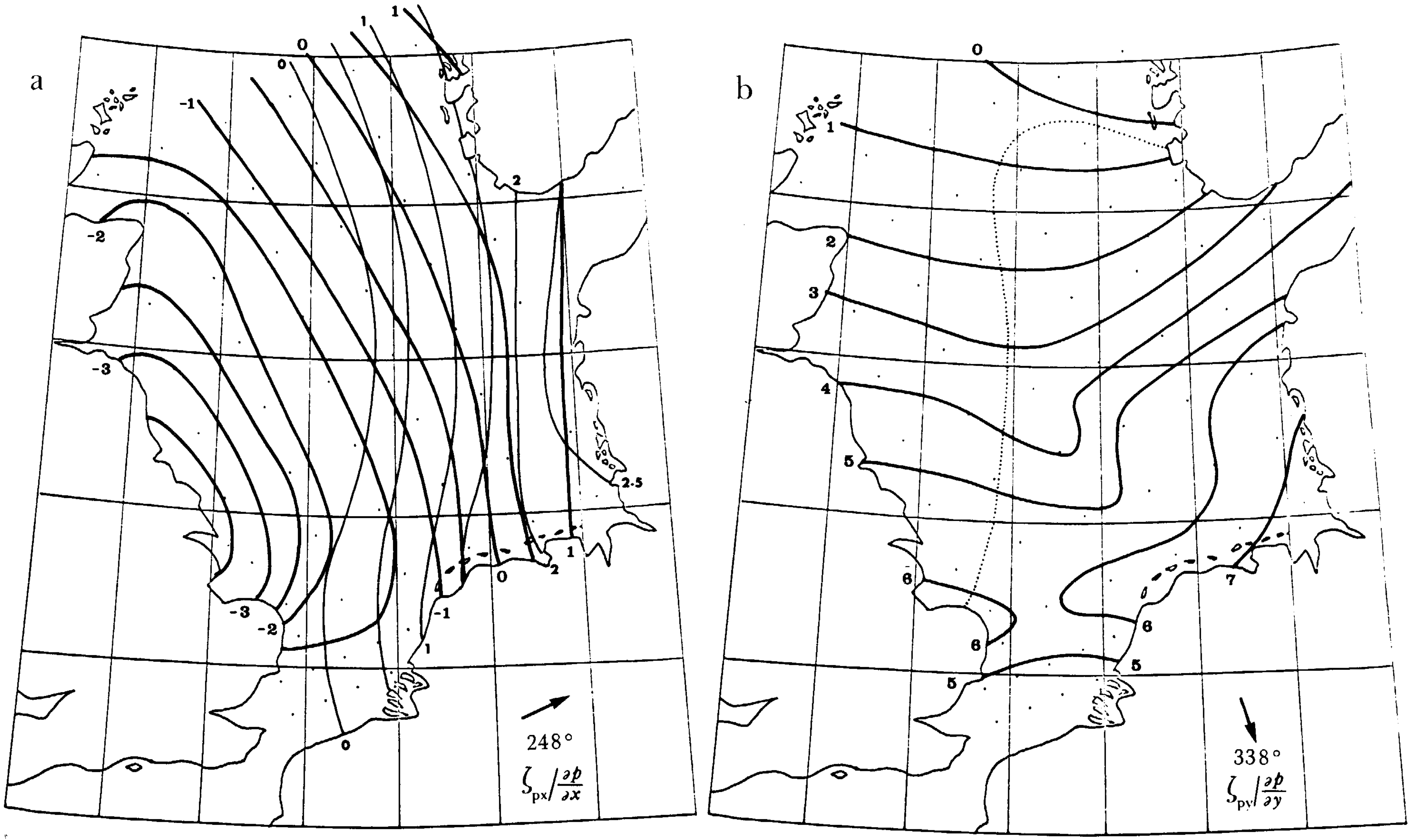


Fig. 2 Diagrams for estimating the equilibrium value (thick line) or peak value (thin line) of the height of a surge, $\zeta_x$ or $\zeta_y$ (cm), generated by a uniform pressure field whose gradient is $\partial p/\partial x$ or $\partial p/\partial y$ (mb/100km) respectively. Line value is in cm/(mb/100km). In the area north of the dotted line, an indistinct peak appears before an equilibrium value, but this can be ignored in most applications.

(3) A set of hydrodynamic equations, representing the North Sea on which a uniform pressure field (constant gradient) is applied instantaneously, and in two rectangular directions, has been solved.

The results are shown in Figs. 2a and 2b. These are indicated by the unit of (surge height)/(pressure gradient) so that the surge height for an arbitrary pressure gradient can be obtained. Let us call them the $\zeta_{px}/\frac{\partial p}{\partial x}$ diagram and $\zeta_{py}/\frac{\partial p}{\partial y}$ diagram.

(4) From the same set of hydrodynamic equations, the regional variations of response time in the sea have been computed, in both rectangular directions.

The results are shown in Figs. 3a and 3b of Ref. 5. Let us call them the $\tau_{px}$ and $\tau_{py}$ diagrams.

(5) Now let us consider meteorological data from which a surge height in the North Sea is estimated. Generally they are statistical data of wind speeds obtained for the North Sea area, typically an extreme value for a certain recurring period, say 50 years. It is important to know how data are derived, particularly the relationship between the wind speed and its averaging period. It is also important to know the size of an area to which such data can be applied. Note that the surge height at a particular position in the sea depends on the pressure and wind fields over the whole sea, as well as those at local area (generally the former is more important).

The data of an extreme wind speed in the North Sea (at the height of 10m above the sea level) for the recurrence period of 50 years has been given by Shellard (1974). This is indicated by a line of constant hourly wind speed in the sea, ranging from 32 m/s (southern part) to 40 m/s (north of the Orkney Islands), with a set of factors by which a wind speed can be converted into another averaging period, as shown in Appendix 2. The relationship between the averaging period, $t_a$ (hours), and the conversion factor, $\alpha$, seems to be exponential, but according to the Meteorological Office, this is 'purely empirical'. Therefore, how far this relationship can be extended, in its speed-averaging period and in the range of wind speeds, is not known to the author, at the moment.

The above mentioned relationship between wind-speed and conversion factor has been interpolated and extended numerically, by the author. Then, this is treated as a continuous function of time, $\alpha(t)$. Another function, $[\alpha(t)]^2$, has also been computed numerically. The values of both the functions are shown in Appendix 2.

(6) If the absolute value of hourly wind speed, $U_1$, is given, therefore, the function, $U_1[\alpha(t)]$ or $U_1[\alpha(t)]^2$ can be obtained shown as in Fig. 3. It is reasonable to assume that a surge whose time constant is $\tau$ is developed by an external force (either pressure gradient or wind stress on the water surface) is maximum at $t = \tau$, as also shown in Fig. 3. $U_1[\alpha(t)]$ should be applied to the wind pressure, and $U_1[\alpha(t)]^2$ should be applied to the wind stress, here.

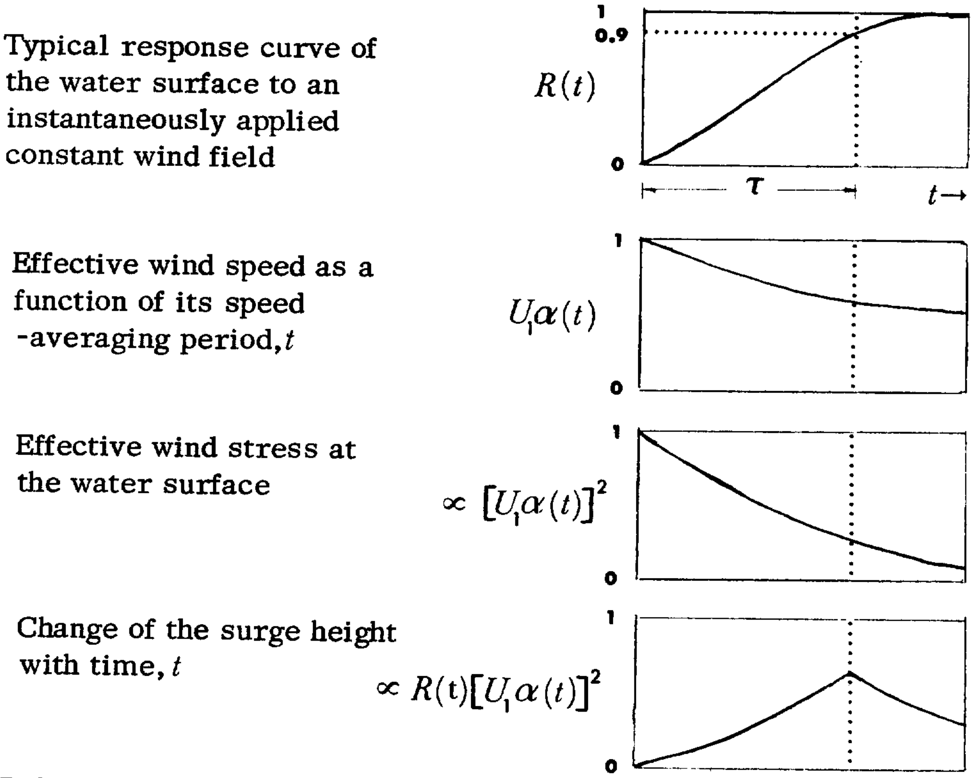


Fig. 3 Relationships between the response time of the water surface and the wind-speed averaging period, in relation to a surge generation.

(7) Since the value of $\alpha(t)$ depends on the type of external force, their direction, and the position in the sea,

$$[\alpha(\tau_{wx})]^2 \equiv \alpha^2_{wx}\ ,\ [\alpha(\tau_{wy})]^2 \equiv \alpha^2_{wy}\ ,\ \alpha(\tau_{px}) \equiv \alpha_{px}\ ,\ \alpha(\tau_{py}) \equiv \alpha_{py}$$

should be applied to the x and y components of wind and pressure fields.

These values have been obtained by combining the relating values previously mentioned. The results are shown in Figs. 4a, 4b, 5a and 5b. Let us call them the $\alpha^2_{wx}$ diagram, $\alpha^2_{wy}$ diagram, $\alpha_{px}$ diagram and $\alpha_{py}$ diagram, respectively.

(8) By multiplying the value for a certain position in the $\zeta_{wx}/u_x^2$ diagram and by that for a corresponding position in the $\alpha^2_{wx}$ diagram, we obtain the value of $\alpha^2_{wx}\zeta_{wx}/u_x^2$ . By applying this method to many positions in the sea, we obtain another diagram as shown in Fig. 6a. Let us call this the $\alpha^2_{wx}\zeta_{wx}/u_x^2$ diagram. In the same way we obtain the $\alpha^2_{wy}\zeta_{wy}/u_y^2$ diagram, as shown in Fig. 6b. Similarly, we obtain the $\alpha_{px}\zeta_{px}/\frac{\partial p}{\partial x}$ diagram and $\alpha_{py}\zeta_{py}/\frac{\partial p}{\partial y}$ diagram, as shown in Figs. 7a and 7b.

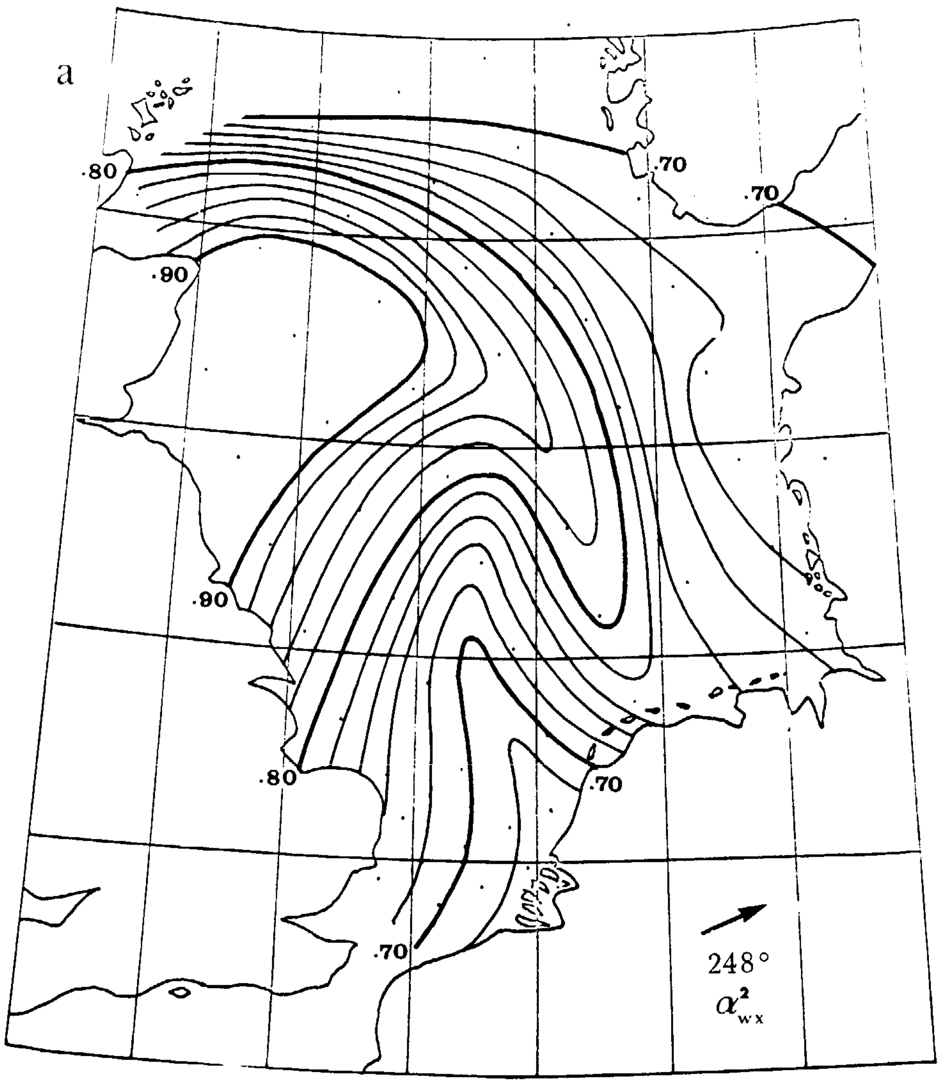


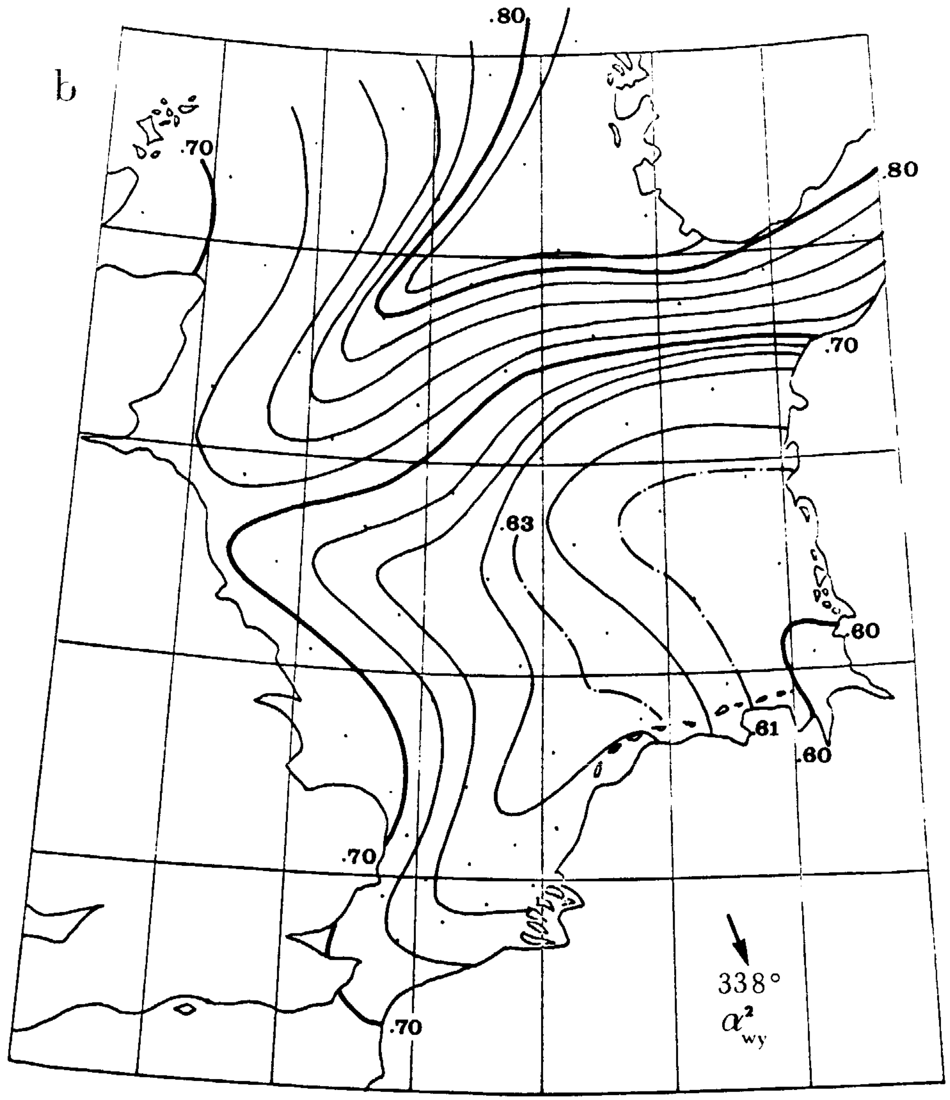


Fig. 4 Diagrams for a factor (dimensionless) to be applied to the height of wind-generated surge. The factor has been derived by combining the sea-surface response time to the wind field, and a factor by which an hourly-mean wind speed is converted into a speed averaged over a period equal to the response time.

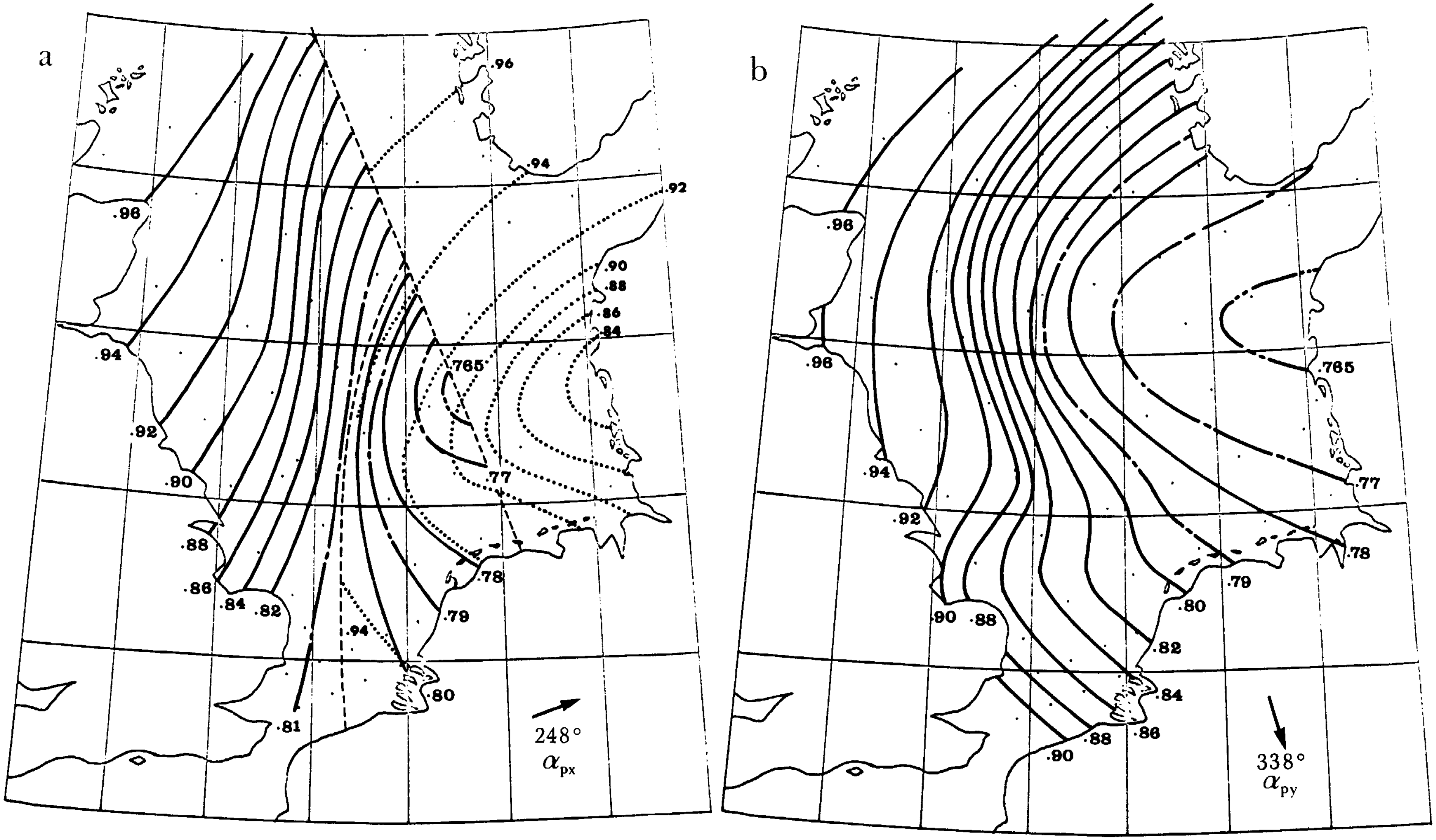


Fig. 5 Diagrams for a factor (dimensionless) to be applied to the height of pressure -generated surge. The factor has been derived by combining the sea-surface response time to the pressure field, and a factor by which an hourly-mean wind speed (relating to the pressure field) is converted into a speed averaged over a period equal to the response time.

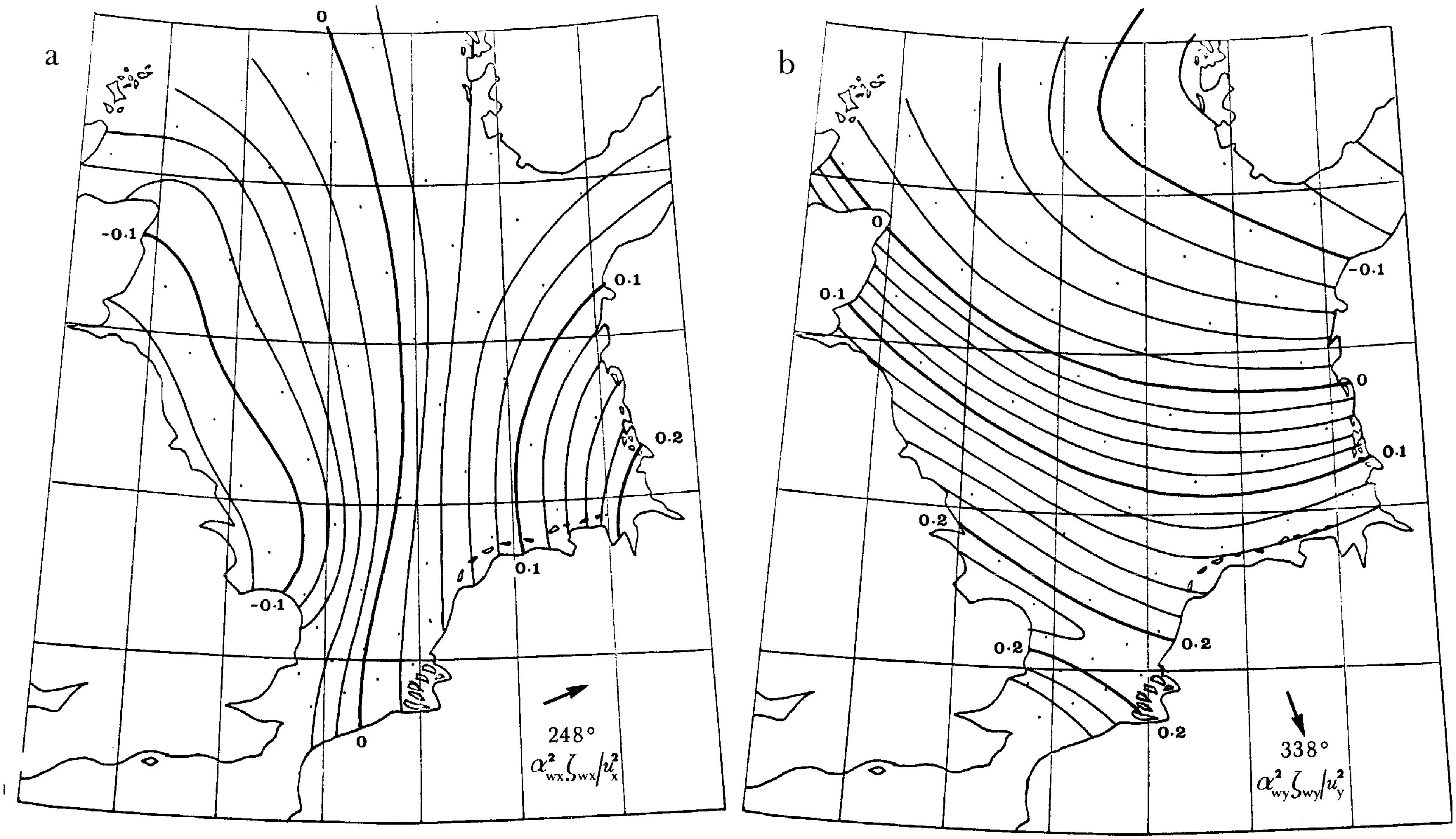


Fig. 6 Diagram for a set of two parameters, relating to a wind-generated surge, from which the highest resultant surge can be estimated, with a similar set for a pressure-generated surge (Fig. 7). Line value is in $m/(m/s)^2$.

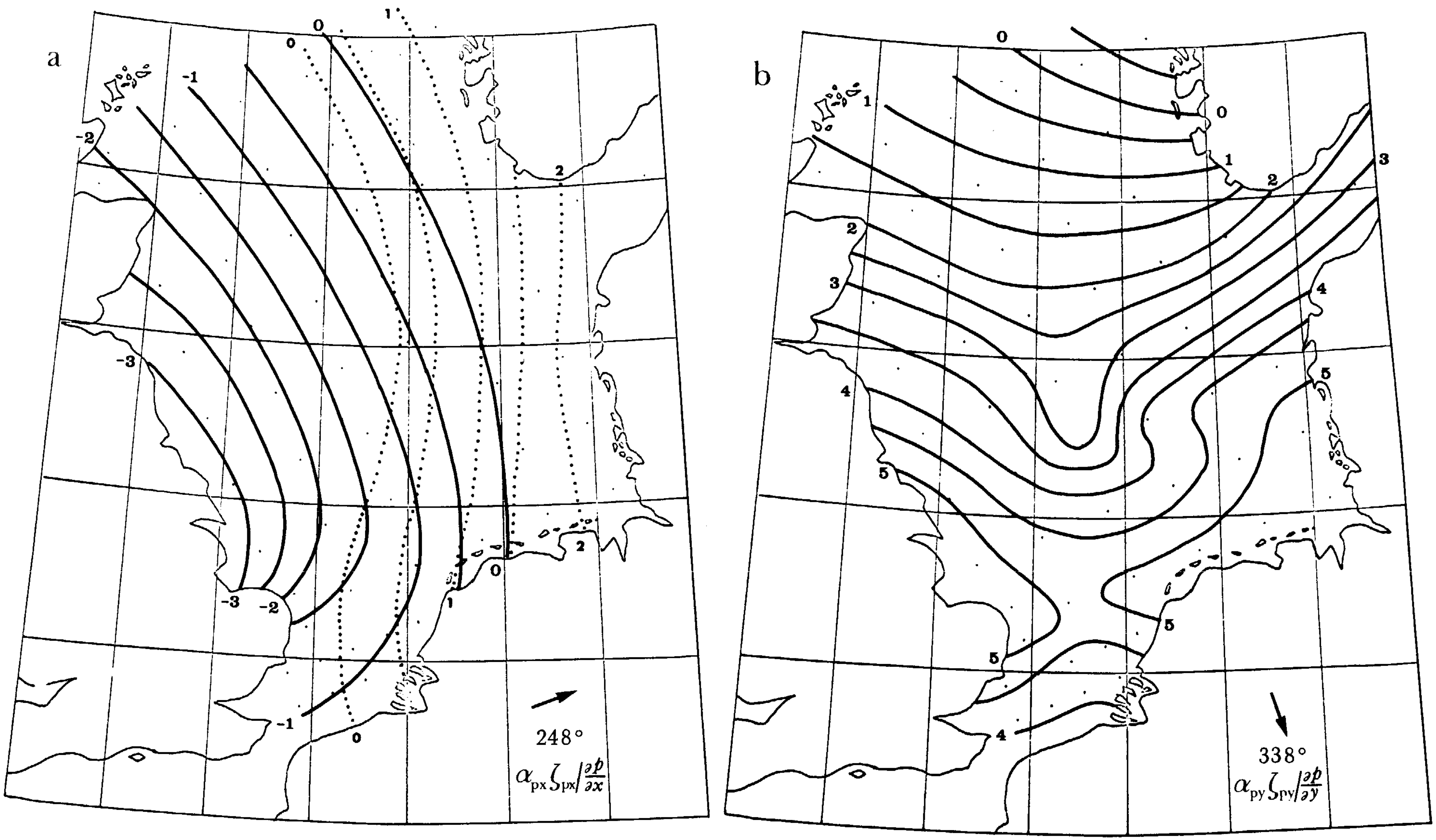


Fig. 7 Diagrams for a set of two parameters, relating to a pressure-generated surge, from which the highest resultant surge can be estimated, with a similar set for a wind-generated surge (Fig. 6). Line value is in $m/(m/s)^2$.

(9) Now a wind field and pressure field must be related in such a manner that both the fields satisfy a single meteorological condition. Among several possible ways of relating them, a set of factors given by Dietrich et al (1952) would be the most appropriate one for this application. They have found, from a large number of observational data in the North Sea for 47 years, that the deflection of wind from the direction of an atmospheric pressure gradient is 77°, and the pressure gradient of 1mb/100km produces the wind speed of 4.5 m/s over most of the sea surface.

By using these data, the gradient, $\partial p/\partial x$ and $\partial p/\partial y$, and the direction of a pressure field referred to that of the wind field, can be determined for a particular hourly wind speed, $U_1$. For example,

$$\frac{\partial p}{\partial x} = \frac{\partial p}{\partial y} = \kappa U_1 = \frac{1\ \text{(mb/100km)}}{4.5\text{(m/s)}} \times U_1 \ \text{m/s} \tag{1}$$

$$\beta = 77° \tag{2}$$

(10) By using the four diagrams, Figs. 6a, 6b, 7a, and 7b, and a particular hourly mean wind speed, $U_1$, we obtain a set of components of a surge height for an arbitrary position in the North Sea, as

$$\bar{\zeta}_{wx} \equiv (\alpha_{wx}^2 \zeta_{wx}/U_x^2) \cdot U_1^2$$

$$\bar{\zeta}_{wy} \equiv (\alpha_{wy}^2 \zeta_{wy}/U_y^2) \cdot U_1^2$$

$$\bar{\zeta}_{px} \equiv (\alpha_{px}^2 \zeta_{px}/\tfrac{\partial p}{\partial x}) \cdot \kappa/U_1$$

$$\bar{\zeta}_{py} \equiv (\alpha_{py}^2 \zeta_{py}/\tfrac{\partial p}{\partial y}) \cdot \kappa/U_1$$

A bar on each symbol here is used only for distinguishing it from similar symbols, and does not have any mathematical meaning, such as 'average'. Each of them could have a positive or negative value which represents water level above or below an undisturbed surface.

(11) The height of a surge at an arbitrary position in the sea can now be obtained by making a vector sum of these four values. Its highest value can also be estimated by taking the maximum value of the vector sum, and the direction of the wind (or pressure gradient) which generates such a height can be obtained from the same set of vector equations.

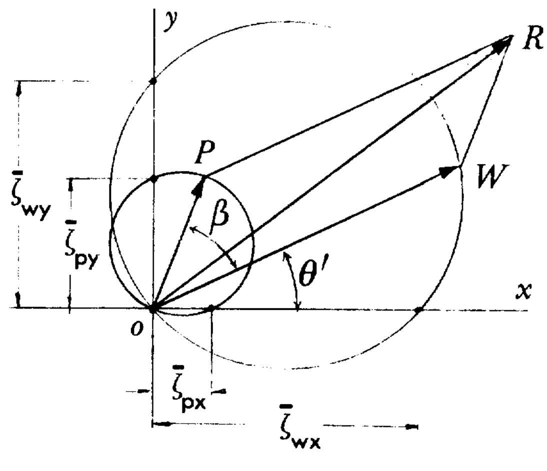


Fig. 8 Vector relationships between four components of a surge height, at a particular position in the sea.

The vector relationships between the four components of a surge height, $\bar{\zeta}_{wx}$ , $\bar{\zeta}_{wy}$ , $\bar{\zeta}_{px}$ and $\bar{\zeta}_{py}$ are shown in Fig. 8., (note that these four components do not have horizontal directions on an actual sea surface), where $W$ is the vector of a wind -generated surge height, whose wind direction is $\theta'$; $P$ is the vector of a pressure -generated surge height, whose direction is $\theta' + \beta$ ; and $R$ is the vector of the resultant surge height of $W$ and $P$, whose height is represented by $\bar{\zeta}_r$. Generally it is convenient to use the direction of wind, $\theta'$, as an indicator of the whole system, when this is referred to geographical north.

The height of the resultant surge is given by

$$\bar{\zeta}_r = \sqrt{m \cos^2 \theta' + n \sin^2 \theta' + q \cos \theta' \sin \theta'} \tag{3}$$

where

$$m = \bar{\zeta}_{wx}^2 + (\bar{\zeta}_{px} \cos\beta + \bar{\zeta}_{py} \sin\beta)^2 + 2\bar{\zeta}_{wx} \cos\beta\, (\bar{\zeta}_{px} \cos\beta + \bar{\zeta}_{py} \sin\beta) \tag{4}$$

$$n = \bar{\zeta}_{wy}^2 + (\bar{\zeta}_{py} \cos\beta - \bar{\zeta}_{px} \sin\beta)^2 + 2\bar{\zeta}_{wy} \cos\beta\, (\bar{\zeta}_{py} \cos\beta - \bar{\zeta}_{px} \sin\beta) \tag{5}$$

$$q = 2\Big[\bar{\zeta}_{wx}\bar{\zeta}_{wy} + (\bar{\zeta}_{px} \cos\beta + \bar{\zeta}_{py} \sin\beta)(\bar{\zeta}_{py} \cos\beta - \bar{\zeta}_{px} \sin\beta) + \bar{\zeta}_{wx} \cos\beta\, (\bar{\zeta}_{py} \cos\beta - \bar{\zeta}_{px} \sin\beta) + \bar{\zeta}_{wy} \cos\beta\, (\bar{\zeta}_{px} \cos\beta + \bar{\zeta}_{py} \sin\beta)\Big] \tag{6}$$

The value of $\theta'$ which makes $\bar{\zeta}_r$ maximum is denoted by $\theta'_{rm}$ , and this is given either by $|\lambda|$ , $90° \pm |\lambda|$ , $180° \pm |\lambda|$ , $270° \pm |\lambda|$ , or $360° - |\lambda|$ (See Appendix 3 for method of determining the correct value), where

$$\lambda = \tfrac{1}{2} \tan^{-1} \left| \frac{q}{m - n} \right| \tag{7}$$

Thus the maximum value of $\bar{\zeta}_r$ is given by

$$\bar{\zeta}_{rm} = \sqrt{m \cos^2 \theta'_{rm} + n \sin^2 \theta'_{rm} + q \cos \theta'_{rm} \sin \theta'_{rm}} \tag{8}$$

Therefore $\bar{\zeta}_{rm}$ and $\theta'_{rm}$ for an arbitrary position in the North Sea for an arbitrary wind speed, $U_l$, can be determined from $\bar{\zeta}_{wx}$ , $\bar{\zeta}_{wy}$ , $\bar{\zeta}_{px}$ and $\bar{\zeta}_{py}$ , when $\beta$ and $\kappa$ are given.

## 4. Applications

How this method would be applied is shown by an example.

Problem: Find the maximum surge height at a position, 54.0°N and 5.0 °E (approximately 100km off the Wash in the North Sea), assuming that an extreme wind over the sea is 36 m/s (hourly mean speed), and also find the wind direction which generates such a surge height.

Solution: Only the four diagrams (Figs. 6a, 6b, 7a and 7b) are needed.

Since $U_1$ = 36 m/s, from Equation 1,

$$\frac{\partial p}{\partial x} = \frac{\partial p}{\partial y} = 36/4.5 = 8.00 \text{ mb/100km}$$

From Fig. 6a, the value for the position is -0.080 cm/(m/s)$^2$

$$\bar{\zeta}_{wx} = -0.080 \times (36)^2 = -103.7\text{cm}$$

From Fig. 6b, similarly,

$$\bar{\zeta}_{wy} = 0.145 \times (36)^2 = 187.9\text{cm}$$

From Fig. 7a, the value for the position is -2.00 cm/(mb/100km)

$$\bar{\zeta}_{px} = -2.00 \times 8.00 = -16.0\text{cm}$$

From Fig. 7b, similarly

$$\bar{\zeta}_{py} = 4.40 \times 8.00 = 35.2\text{cm}$$

Taking $\beta$= 77°, cos$\beta$= 0.225, and sin$\beta$ = 0.974,
For Equations 4, 5, 6,

$$\bar{\zeta}_{px}\cos\beta = -16.0 \times 0.255 = -3.6 \text{ cm}$$

$$\bar{\zeta}_{px}\sin\beta = -16.0 \times 0.974 = -15.6\text{cm}$$

$$\bar{\zeta}_{py}\cos\beta = 35.2 \times 0.225 = 7.9\text{cm}$$

$$\bar{\zeta}_{py}\sin\beta = 35.2 \times 0.974 = 34.3\text{cm}$$

$$\bar{\zeta}_{px}\cos\beta + \bar{\zeta}_{py}\sin\beta = -3.6 + 34.3 = 30.7\text{cm}$$

$$\bar{\zeta}_{py}\cos\beta - \bar{\zeta}_{px}\sin\beta = 7.9 + 15.6 = 23.5\text{cm}$$

From Equations 4, 5, and 6,

$$m = (-103.7)^2 + (30.7)^2 + 2(-103.7) \times 0.225 \times 30.7 = 10264\text{cm}^2$$

$$n = (187.9)^2 + (23.5)2 + 2(187.9) \times 0.225 \times 23.5 = 37846\text{cm}^2$$

$$q = 2[(-103.7 \times 187.9) + (30.7 \times 23.5) + (-103.7 \times 0.225 \times 23.5) + (187.9 \times 0.225 \times 30.7)]$$

$$= -36028\text{cm}^2$$

From Equation 7,

$$\lambda = \tfrac{1}{2}\tan^{-1}\left|\frac{-36028}{10264 - 37846}\right| = 26.3°$$

From Appendix 3,

$$\theta'_{rm} = 90.0° + 26.3° = 116.3°$$

For Equation 8, $\cos^2\theta'_{rm} = 0.196$, $\sin^2\theta'_{rm} = 0.804$, $\cos\theta'_{rm} \times \sin\theta'_{rm} = -0.397$

From Equation 8,

$$\bar{\zeta}_{rm} = \sqrt{(10264 \times 0.196) + (37846 \times 0.804) + (-36028 \times -0.397)} = 216.2 \text{ cm}$$

The value of $\theta'_{rm}$ here is referred to the x and y axes of each grid of the model. In order to convert this value into a wind direction, $\theta_{rm}$, (the direction from which the wind is blowing) referred to geographical north, the following equation must be used.

$$\theta_{rm} = \theta'_{rm} - \epsilon - 90° \tag{9}$$

where $\epsilon$ is an angle specified for each grid, and -90° is a constant specified for the system by which the polarities of water level and the direction of wind and pressure gradient are related, throughout this paper. The value of $\epsilon$ for the North Sea is shown in Appendix 1.

The value of $\theta'_{rm}$ obtained in the above example is now converted by using Equation 9 and the value of $\epsilon$ for this position, 22.8°, as

$$\theta_{rm} = 116.3° - 22.8° - 90° = 3.50°$$

The final answer to the problem is therefore

> 'The highest surge at the given position will be 216 cm above a predicted tidal level, and the direction of wind which generates such a surge will be 3.5° (approximately N), referred to geographical north.'

The calculations shown in this example have been carried out by a pocket calculator with memory, taking about 10 minutes. Approximate calculations for this can be done by a simplified way, or by graphical calculations, using a similar graph to Fig. 8. Note that calculations of the angle in Equation 7 should be accurate, otherwise an error will be introduced at this stage.

See Fig. 9 for the diagram which has been obtained by applying this method of calculation to the whole area of the North Sea for a proposed extreme wind speed for the average recurrence period of 50 years.

## 5. Comparisons of results

The highest surge in the whole area of the North Sea, under a certain wind speed, estimated by the same procedure as the example in Chapter 4, is described here, in comparison with some special cases and a similar estimation obtained by the orignal method (outlined in Chapter 2).

Fig. 9 shows the result of the estimated highest surge in the North Sea, by the improved method, for the hourly-mean wind speed of 38 m/s over the sea, and the direction of wind which generates such a surge. Note that the estimated values cannot be extended to other wind speeds, since their relationships are not linear in this method. An area in which the surge height is minimum under any direction of wind field (and that of its associate pressure field) appears in the centre of the sea, as this has been described in earlier paper (Ishiguro, 1966). The minimum here, however, is not zero due to the pressure field being taken into account. The maximum value of the highest surge throughout the North Sea appears in the Wash under the wind direction of 360°, and in the German Bite under the wind direction of 280°.

### 5.1 Effect of the pressure field in a high wind speed

In order to examine the contribution of the pressure field to the generation of the highest surge at an arbitrary position in the sea, the same computations as for Fig. 9, but without the pressure terms, have been carried out. The result obtained is so similar to Fig. 9 that any difference can hardly be recognised from their contour maps (the diagram for the former is, therefore, omitted from this paper). The difference between the computations with and without the pressure field can be expressed by

$$\Delta\bar{\zeta} \equiv \bar{\zeta}_{rm} - \sqrt{\bar{\zeta}^2_{wx} + \bar{\zeta}^2_{wy}}$$

and

$$\Delta\theta \equiv \theta'_{rm} - \tan^{-1}(\bar{\zeta}_{wy} / \bar{\zeta}_{wx})$$

(see Procedure 10 and Equation 8 for the notations of symbols).

Fig. 10a shows a contour map of $\Delta\bar{\zeta}$, Fig. 10b shows $\Delta\bar{\zeta}/\bar{\zeta}_{rm}$ and Fig. 10c shows $\Delta\theta$. We understand, from these diagrams, that the effect of a pressure field on the generation of the highest surge is significant only in the south-eastern part of the North Sea (approximately a quarter of the whole sea area). The pressure field increases the maximum surge height of 120cm in this area by 17cm, or 15%. In the rest of the North Sea, the pressure field changes the surge height within ± 2%. The effect of the pressure field on the wind direction, $\theta_{rm}$, is not significant throughout most of the North Sea.

This suggests that a set of simplified calculations

$$\bar{\zeta}_{rm} \simeq \sqrt{\bar{\zeta}^2_{wx} + \bar{\zeta}^2_{wy}}$$

$$\theta'_{rm} \simeq \tan^{-1}(\bar{\zeta}_{wy} / \bar{\zeta}_{wx})$$

which takes less than one minute using a pocket calculator, is sufficient for most applications.

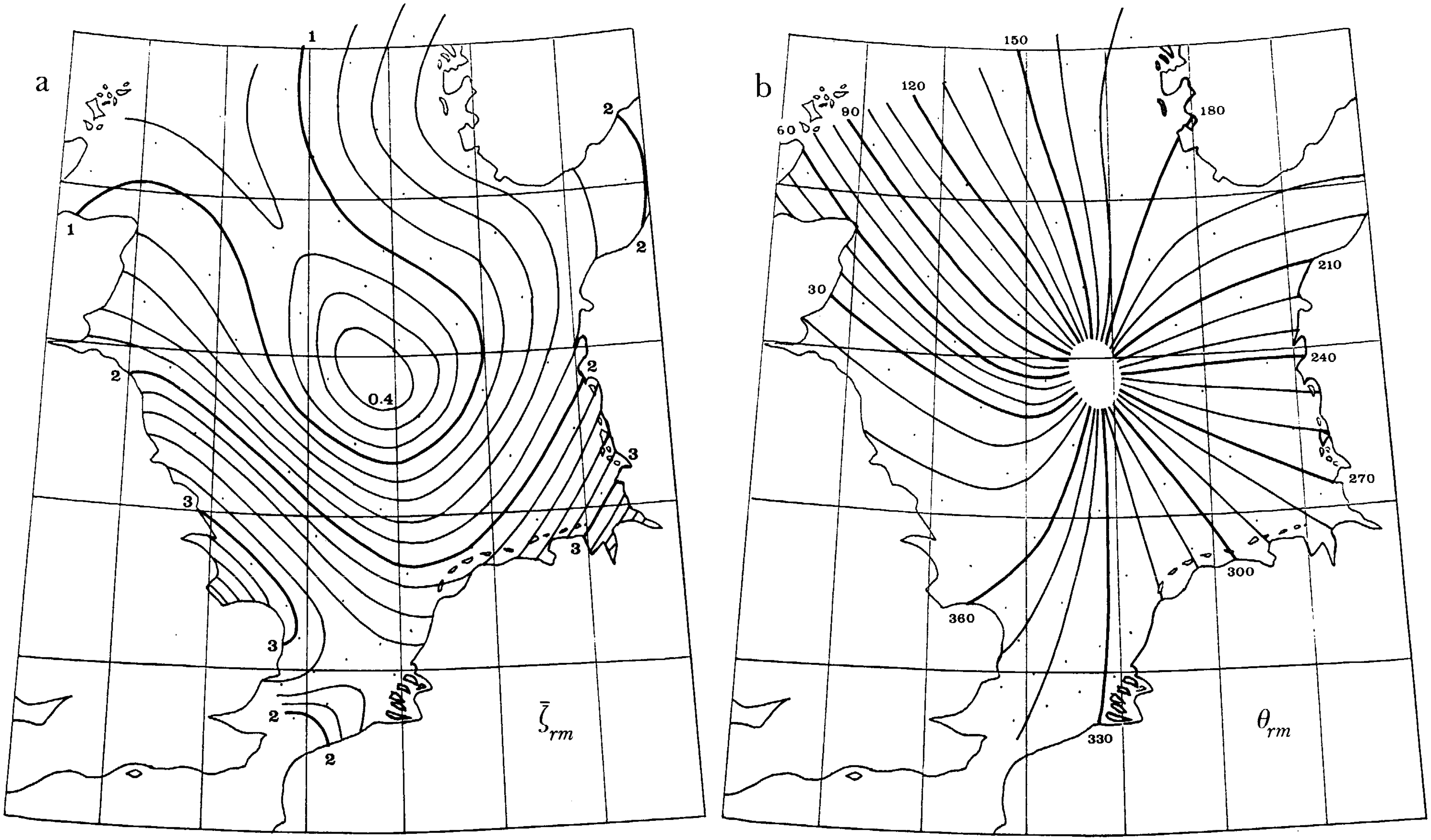


Fig.9 Diagrams for estimating the highest surge (generated by a wind field and pressure field) at an arbitary position in the North Sea for the hourly-mean wind speed of 38m/s (a proposed extreme wind speed for the average recurrence period of 50 years), produced by the improved method. Line value in (a) is surge height, in metres, and that in (b) is the direction of wind, in degrees, by which such a surge is generated.

The reasons why the pressure field does not significantly affect an estimated surge height in the North Sea, with a high wind speed, can be explained as follows.

(1) The effect of the pressure field on the surge is proportional to its gradient, which is proportional to the wind speed, while the effect of the wind field is proportional to the square of its speed.

(2) The directional effect of a wind field and that of a pressure field on the general patterns of a surge in the North Sea are similar, if each field is applied separately, since the patterns are mainly determined by the bottom topography of the sea (compare Fig. 1 and Fig. 2 ). In fact, the directions of the two fields are considerably different (77° in this example), therefore when the wind field is in the most effective direction for surge generation, its associated pressure field is not in an effective direction.

## 5. 2 Effect of the pressure field in a low wind speed

The relationships between the pressure field and its associated wind field, described in the previous paragraph, would be somewhat changed when the wind speed is low (say 10 m/s).

Table 1 shows an example of this situation, although the degree of the change depends on the value of the wind speed and the position in the sea. For this example, the same position in the sea as that for the example in Chapter 4 is used.

Table 1. Examples of the effect of the pressure field on the estimated highest surge, under different wind speeds, at a certain position of the North Sea (54. 0°N, 5. 0°E).

| Hourly-mean wind speed | m/s | 10 | 20 | 36 |
|---|---|---|---|---|
| Highest surge estimated by the full computations | cm | 17. 5 | 67. 3 | 216. 2 |
| The same, but without a pressure field | cm | 16. 1 | 66. 2 | 214. 6 |
| Difference, referred to the full computations | cm<br>% | 0. 9<br>5. 1 | 1. 1<br>1. 6 | 1. 6<br>0. 7 |
| Wind direction, estimated by the full computations | deg. | -12. 26 | 0. 71 | 3. 50 |
| The same, but without a pressure field | deg. | 6. 09 | 6. 09 | 6. 09 |
| Difference, referred to the full computations | deg. | -16. 35 | -5. 38 | -2. 59 |

a

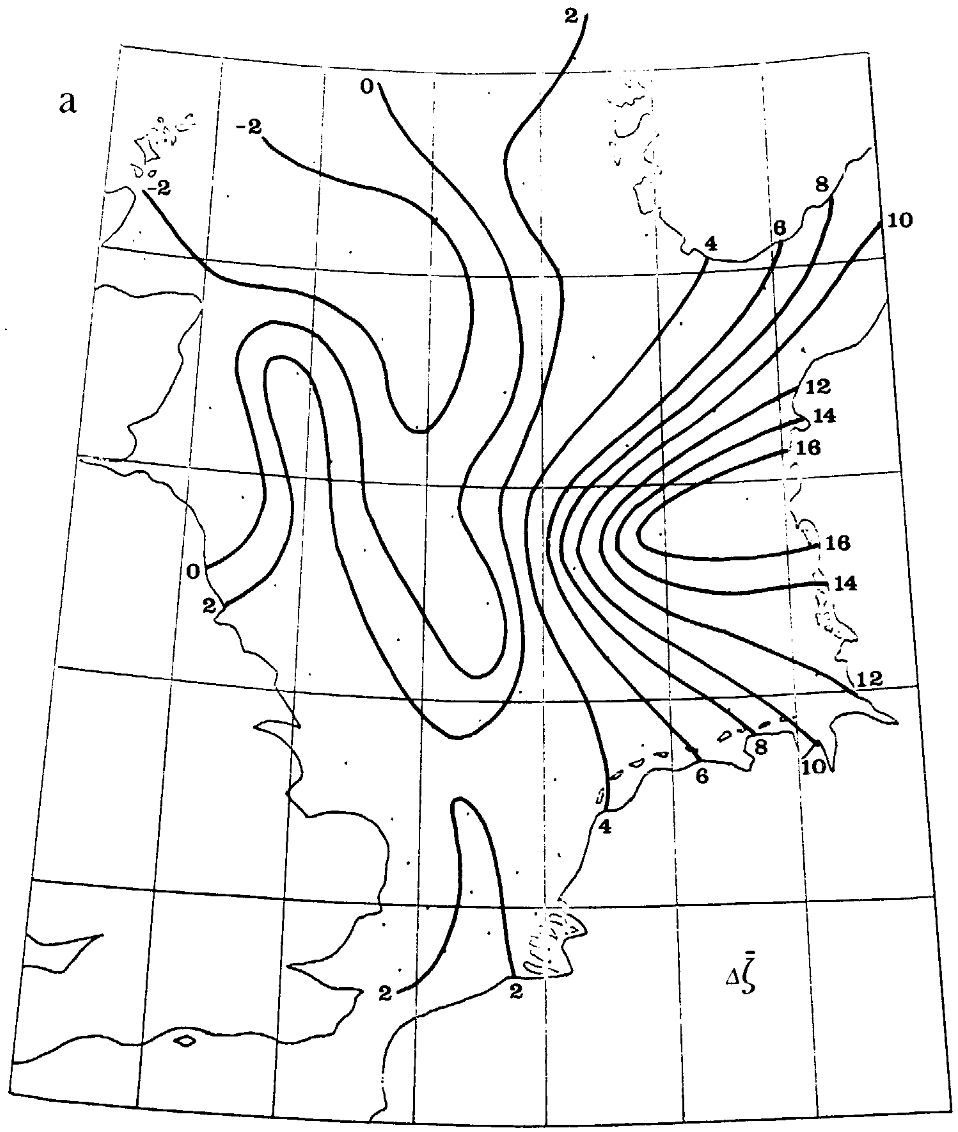


b

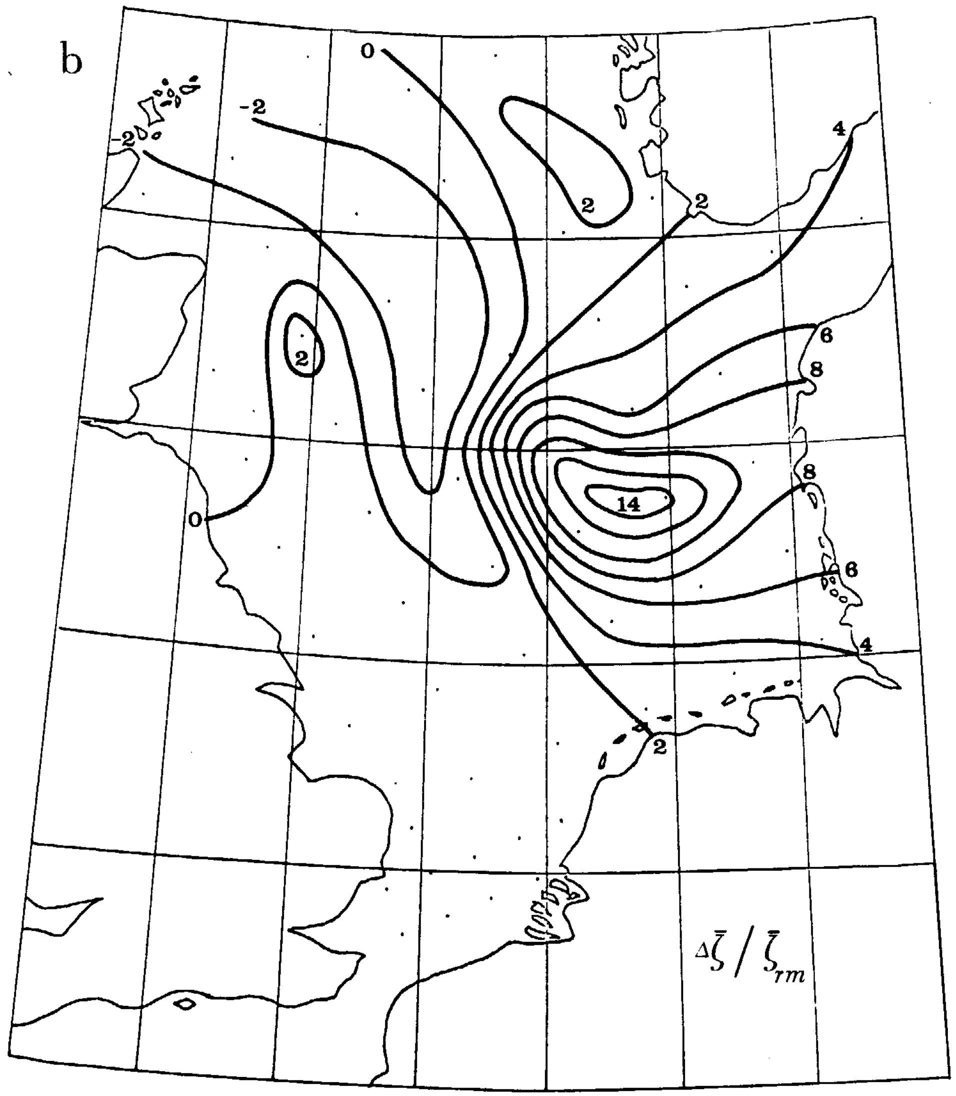


Fig. 10 (a) Difference in the highest surge estimated by the full computations and computations without a pressure field both by the improved method. Line value is in cm.

(b) The same as Fig.10(a), but with the percentage of the fully computed value.

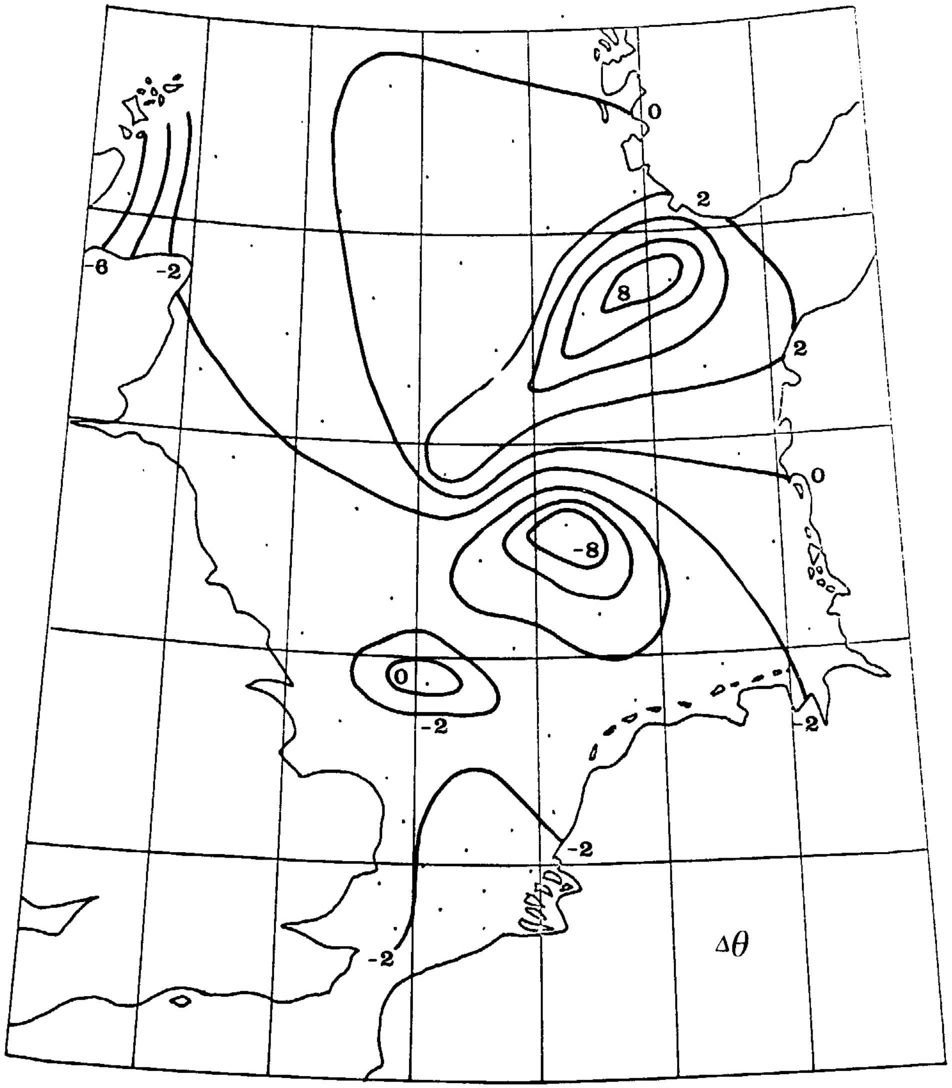


Fig. 10c Difference in the wind direction, in degrees, by which the highest surge is generated at each position in the North Sea, estimated by the full computations and those without a pressure field, both by the improved method.

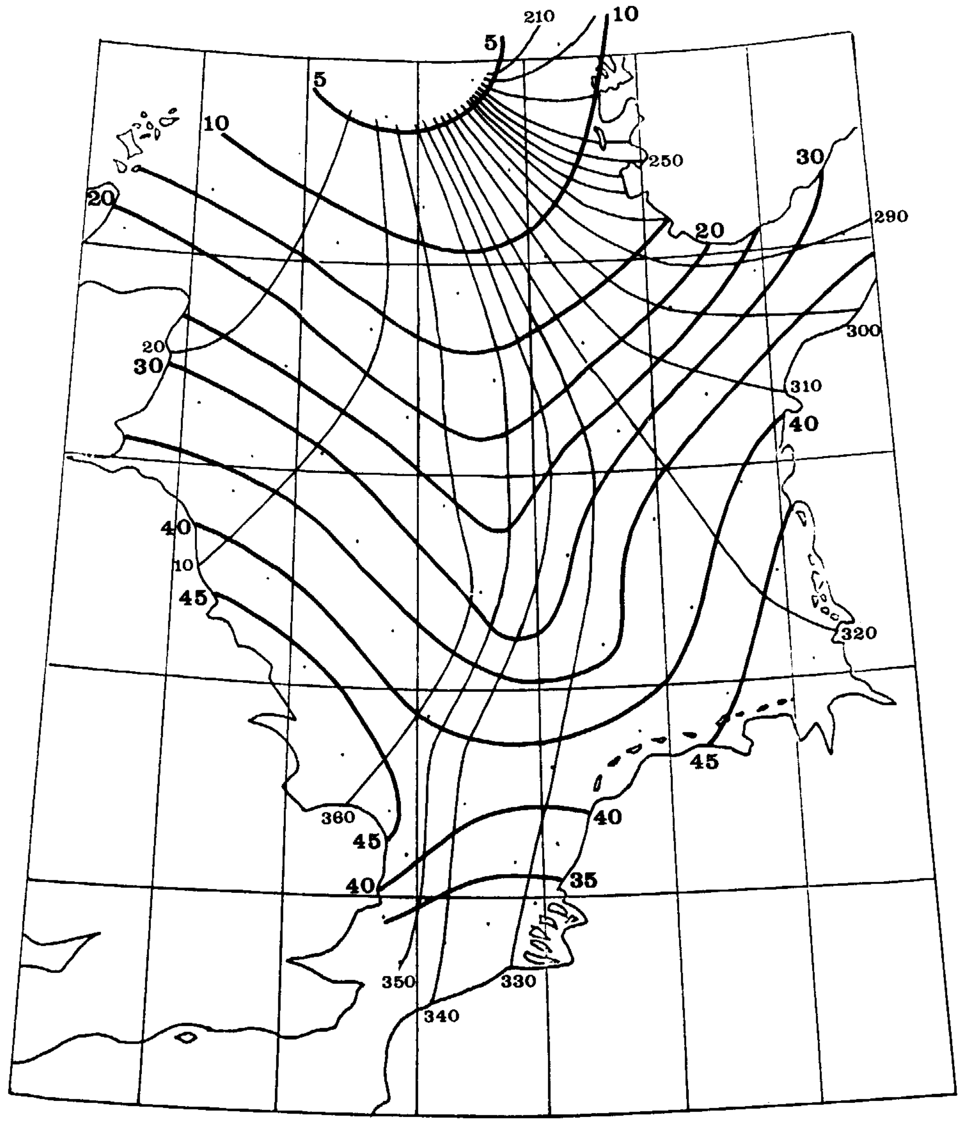


Fig. 11 The diagram for estimating the highest surge in the North Sea, generated solely by a uniform pressure field, produced by the improved method.
Thick line: surge height in cm/(mb/100km).
Thin line: direction of wind, in degrees.

## 5.3 Effect of the pressure field in the south-eastern part of the North Sea

In Figs. 10a and 10b, a relatively significant effect of the pressure field on the surge height can be seen in the south-eastern part of the North Sea. This can be explained as follows:

(1) The maximum value of $\Delta\bar{\zeta}$ appears off Esbjerg (in Fig. 10a), and its corresponding $\theta_{rm}$ at this position is 240° (in Fig. 9b). When the pressure field is omitted from the computation, this value reduces to 236°. The direction of the pressure field which is associated with this value is 169°. For a pressure field in such a direction, the maximum surge generated solely by it is coincidentally off Esbjerg (see the 248° diagram and 278° diagram in Fig. 4 of Ref. 5).

(2) The maximum of $\Delta\bar{\zeta}/\bar{\zeta}_{rm}$ appears about 150km west of Esbjerg, because the gradient of $\bar{\zeta}_{rm}$ toward the continental coast is greater than that of $\Delta\bar{\zeta}$ .

Although the irregularity of $\Delta\bar{\zeta}$ in the rest of the North Sea can be explained in a similar way, its magnitude is not significant.

## 5.4 Highest pressure-generated surge

This has been discussed in another paper (Ishiguro, 1976) by using the original method. The same treatment, but by the improved method, is carried out here, in order to examine the difference with a pressure field alone. Such a condition can be obtained by computing

$$\bar{\zeta}_{pm} = \sqrt{\zeta_{px}^2 + \zeta_{py}^2}$$

$$\theta'_{pm} = \tan^{-1}(\bar{\zeta}_{py} / \bar{\zeta}_{px})$$

Fig. 11 shows the result. This diagram should be compared with Fig. 5 of the previously mentioned paper. Although they are similar, a significant difference can be seen in an area bounded by the 0° (or 360°) line and 340° line. The area bounded by the 0° line and 320° line is considerably compressed, and the area bounded by the 320° line and 340° line is expanded, while these areas are almost uniformly divided in the result from the other paper.

The reason for this can be explained as follows. In the improved method, the height of a peak, which appears before the equilibrium value and is higher than it, is detected as the highest surge value. In the original method, the highest surge value at a particular instant (the 10th hour for this example) is regarded as the highest surge. Obviously the former is correct.

### 5.5 Comparisons with the original method

The highest surge in the North Sea estimated by the improved method and that by the original method are compared here, under similar conditions (exactly the same conditions cannot be given to the two methods, because their required conditions are not the same).

For an example of estimation by the original method, the wind speed of 36 m/s and the wind duration of 10 hours are given. These values are related to the hourly -mean wind speed of 38 m/s and a speed reduction factor of 0.885 for the speed -averaging period of 10 hours. Figs. 12a and 12b show the results, where $\bar{\zeta}_0$ indicates surge height, $\theta_0$ the direction of wind generating such a surge. These values are compared with the corresponding values to these in Figs. 9a and 9b, i.e. $\bar{\zeta}_{rm}$ and $\theta_{rm}$, by taking $\bar{\zeta}_{rm} - \bar{\zeta}_0$ and $\theta_{rm} - \theta_0$ respectively, as shown in Figs. 13a and 13b.

In Fig. 13a, the value of $\bar{\zeta}_{rm} - \bar{\zeta}_0$ is positive throughout the North Sea, with an average value of approximately 20cm, the maximum value being 140cm along the Dutch coast. This considerable difference is not due to the omission of a pressure field from the original method (because these do not appear in Fig. 10a), but due to the introduction of $\alpha^2_{wx}$ and $\alpha^2_{wy}$, (see Fig. 4) into the improved method. By using these terms, a combined effect of the response time of the sea surface and the wind-speed averaging period, which determines the highest surge more precisely than the original method, can be taken into account.

In Fig. 13b, the value of $\theta_{rm} - \theta_0$ is zero along a line passing the centre of the sea in north-south direction approximately. The value is negative on the British side of this line, and positive on the continental side. The difference is within ±20 degrees. Although this is still small compared with 360°, it is significantly greater than the difference in Fig. 10c. This difference is, therefore, again due to the introduction of $\alpha^2_{wx}$ and $\alpha^2_{wy}$ into the improved method.

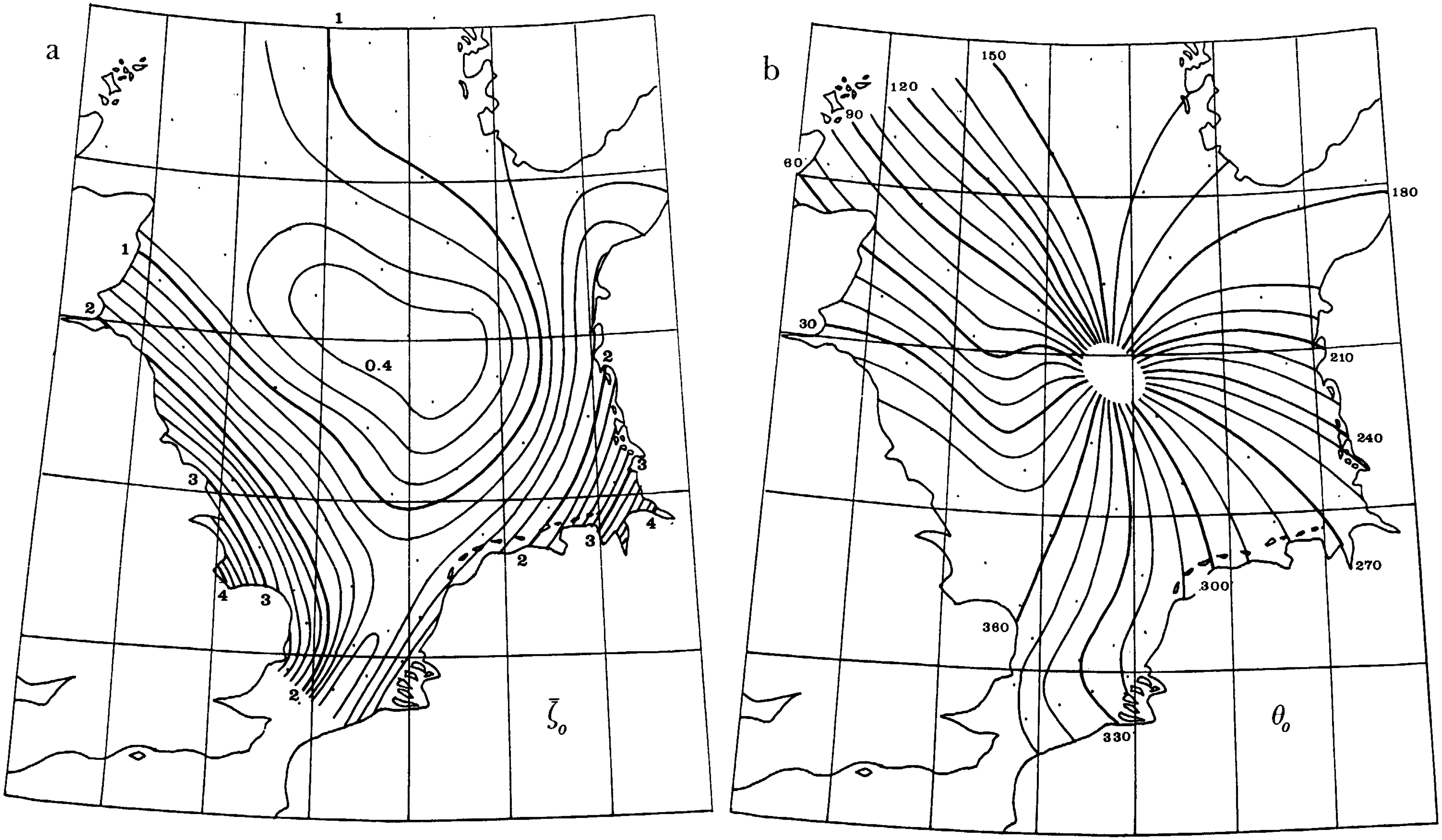


Fig. 12 Diagram for estimating the highest surge at an arbitrary position in the North Sea, for the wind speed of 36 m/s averaged over its duration of 10 hours, produced by the original method for the comparison with Fig. 9. Line value in (a) is the surge height in metres, and line value in (b) is the direction of wind, in degrees, by which such a surge is generated.

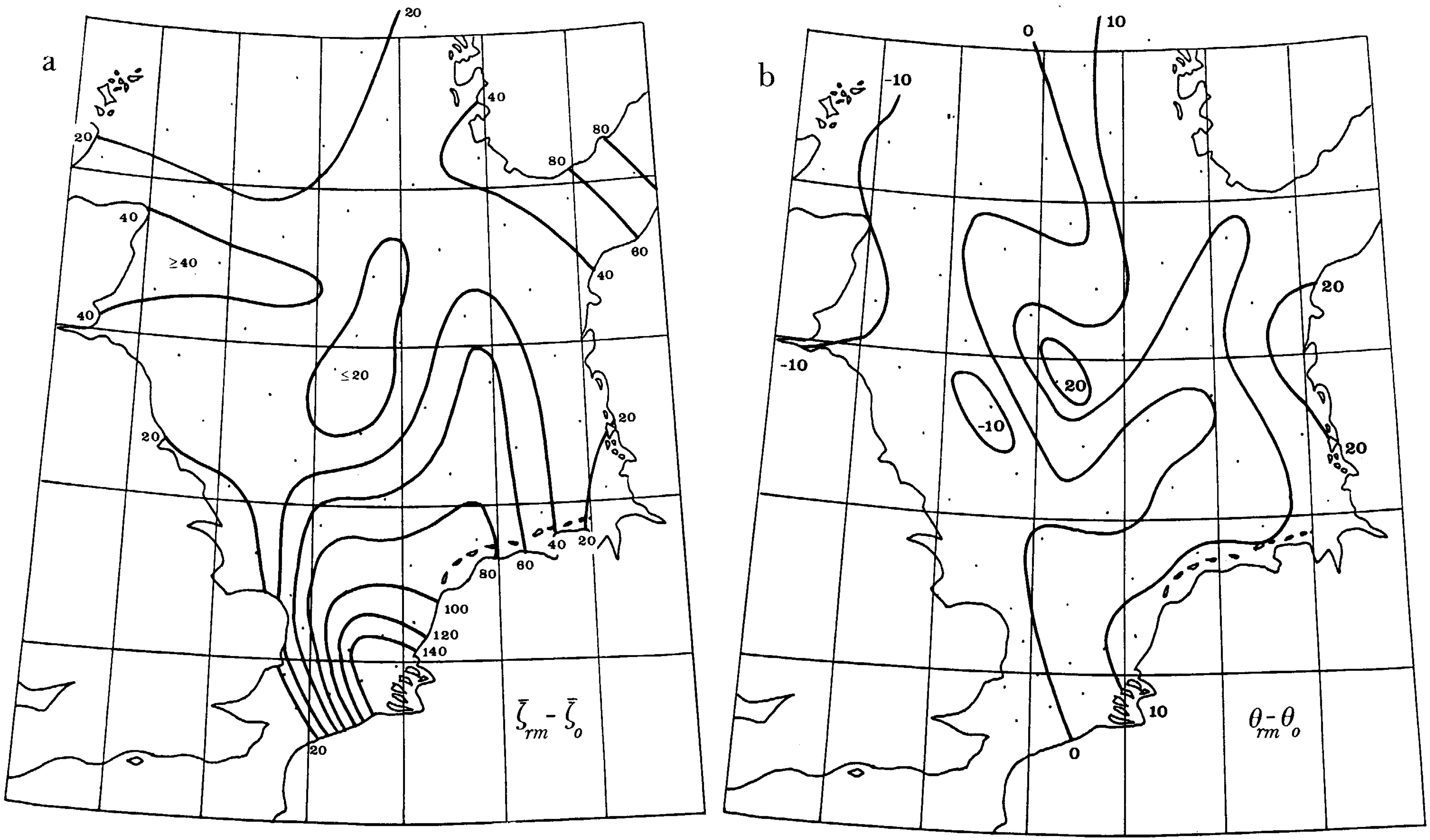


Fig. 13 Comparison between the highest surge in the North Sea estimated by the improved method and original method. Line value in (a) is the difference in surge height in cm, and line value in (b) is the difference in degrees.

## 6. Conclusions

A practical method of estimating the highest storm surge in the North Sea under a given wind speed has been made. Two sets of hydrodynamic computations for wind-generated surge and pressure-generated surge, each having two rectangular directions (i. e. four cases in all), are made in the form of 'equal-value line' maps (Figs. 6 and 7). Four parameters are selected from them for a position in the sea, for which an estimation is required, and each of the values are adjusted for the given wind speed. The maximum value of their vector sum gives the highest surge and the direction of wind by which such a surge is generated. The full vector calculations take about 10 minutes using a pocket calculator, and the simplified calculations which still have a fairly reasonable accuracy for most applications take less than one minute.

In this method, the response time of the sea surface (which varies with a position in the sea and the direction of an external force) and the wind-speed factor (which reduces with its speed-averaging period) are combined so that the highest surge can be determined from the hourly-mean wind speed, without being affected by an estimated duration of wind.

As an example, a diagram indicating the highest surge for the whole area of the North Sea under a certain wind speed (a proposed extreme wind speed for the average recurrence period of 50 years) has been made. This diagram has been analysed by comparing with some special cases, such as that without a pressure field, and a similar diagram obtained by another method (Ishiguro, 1966). The analysis shows:

(1) For a high wind speed (say 38 m/s in hourly-mean value), the error, in the estimated surge height, due to the omission of a pressure generated surge is generally negligible, except for a particular part of the North Sea.

(2) For a low wind speed (say 10 m/s), the effect of a pressure field becomes more significant (say 15% in height, and 16° in wind direction), depending on a position in the sea.

(3) The maximum surge height, under a constant wind speed of any direction, reduces toward the centre of the North Sea, where the surge height is minimum, although not zero. Note that another computation without pressure field (Ref. 2) shows a similar area in the centre of the sea, but with zero height.

(4) Even in a high wind speed, the effect of a pressure field is noticable, in the south -eastern part of the North Sea (maximum 14% in height, and ±8° in wind direction). The pressure field contributes in reducing the highest surge around the Scottish coast, but increasing it in the rest of the North Sea. The pressure field generally has little effect on the wind direction by which such a surge is generated.

(5) New factors, $\alpha_{px}$ etc., introduced into this method detect the highest surge, in relation to the response time of the sea and wind-speed averaging period, as well as its equilibrium value; for example a peak which appears before it.

The accuracy of this method mainly depends on that of the two sets of hydrodynamic computations from which the basic four parameters are derived, as well as the accuracy of estimated meteorological conditions. All the dynamic computations used in this paper have been computed by the electronic model, whose accuracy has been proved to be reasonable by comparing its output with observational data of tides and storm surges in the North Sea (ref. 4).

Although the highest surge estimated by this method should also be compared with observational data in the sea, the history of observations is very short, particularly those for offshore, compared with the recurrent period of an extreme value in question (say 50 years).

Nevertheless, this paper hopefully gives some information on the characteristics of the highest surge in the North Sea, in addition to its estimated values.

Further improvements of the method, including treatments of so-called external surges which are omitted from this paper, are expected by using the newly built electronic model.

## Acknowledgement

The author is grateful to Mr. Patrick Doncaster for his help with numerical computations used in Chapter 5.

## References

(1) Dietrich, G. et al (1952)
Wind conditions over the sea around Britain during 1900-1946, The German Hydrographic Institute, Hamburg, pp. 38.

(2) Ishiguro, S. (1966)
Storm surges in the North Sea, Advisory Committee on Oceanographic and Meteorological Research, Paper 25 (iii) pp. 57.

(3) Ishiguro, S. (1967)
Storm surges in the North Sea, Advisory Committee on Oceanographic and Meteorological Research, Paper 27 (iii) pp. 97.

(4) Ishiguro, S. (1972)
An electronic model for tides and storm surges in the North Sea, IOS Internal Report, pp. 234.

(5) Ishiguro, S. (1976)
Pressure-generated surge in the North Sea, IOS Internal Report No. 35, pp. 26.

(6) Shellard, H. C. (1974)
Proposed revision of extreme wind maps, Meteorological Office, Unpublished (for publication in revised Guidance Notes, Department of Energy).

## Appendix 1 Indication of directions

The wind direction is customarily specified as that direction from which the wind is blowing. When this is indicated by an angle, it increases clockwise, referred to geographical north. This system is used, in this paper, for indicating a wind direction, and the direction of a pressure gradient (toward its low pressure), for convenience in treating their surge generations.

For a mathematical expression, the right-hand rectangular cartesian co-ordinate system, in which an angle increase anticlockwise, referred to its positive x-axis is used in this paper, the x and y components of each grid of the model being referred.

Each axis of model grids covering a large area has a different angle referred to geographical north. The angle of the y-axis referred to geographical north is denoted by $\epsilon$, and the variations of this value in the North Sea are shown in the left diagram.

The indication of directions is also related to the system by which the polarities of water level and the directions of wind and pressure gradient are related.

Equation 9 has been derived from these conditions.

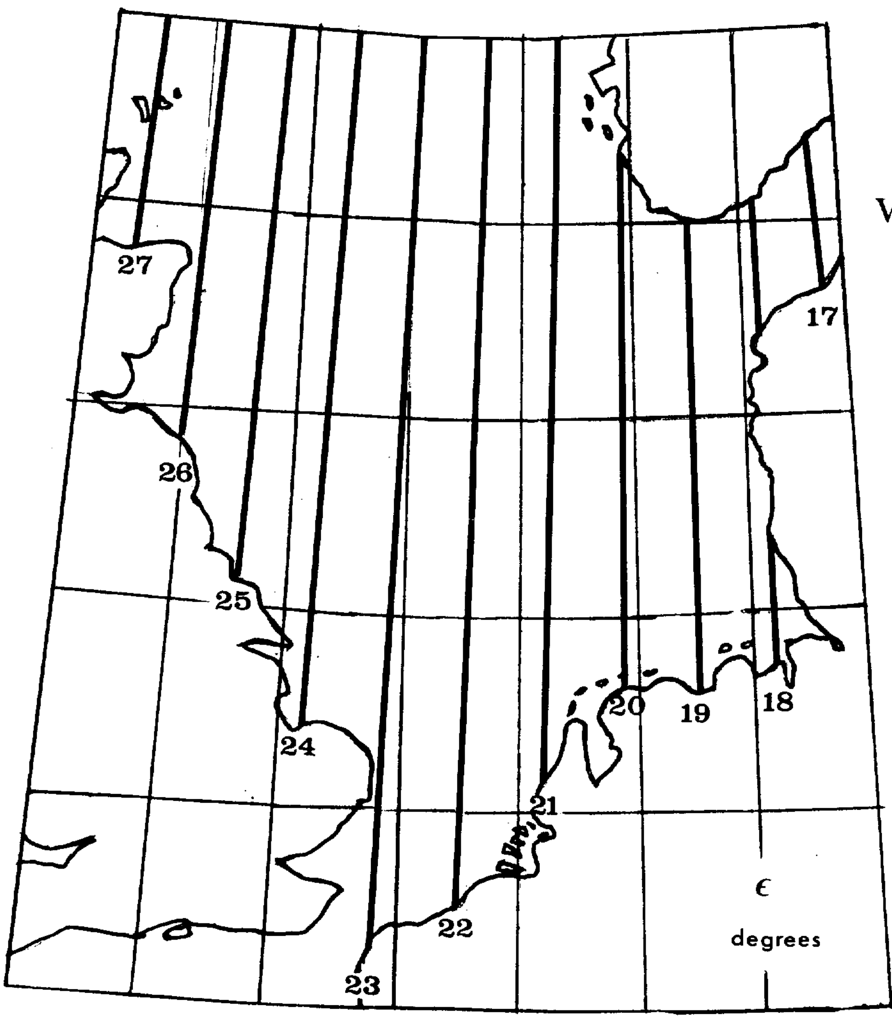


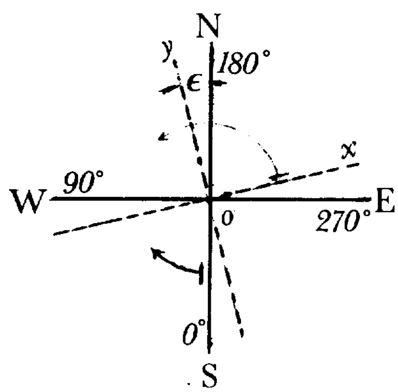


0° is taken in S-direction, in order to indicate a wind direction in the same manner as other factors.

Appendix 2 Values of $\alpha$ and $\alpha^2$ in Procedure 7 (Page 8)

Table 1 Original value of $\alpha$, by Shellard (1974)

| Wind-speed Averaging period $t$ hours | Factor $\alpha$ |
|---|---|
| 1 | 1.00 |
| 3 | 0.96 |
| 6 | 0.93 |
| 12 | 0.87 |
| 24 | 0.80 |

Table 2 Expanded values of $\alpha$, by the author

| $\alpha$ | $t$ hours |
|---|---|
| 1.00 | 1.0 |
| 0.99 | 1.4 |
| 0.98 | 1.7 |
| 0.97 | 2.3 |
| 0.96 | 3.0 |
| 0.95 | 4.0 |
| 0.94 | 5.0 |
| 0.93 | 6.0 |
| 0.92 | 7.0 |
| 0.91 | 7.9 |
| 0.90 | 8.9 |
| 0.89 | 9.9 |
| 0.88 | 10.9 |
| 0.87 | 11.0 |
| 0.86 | 13.3 |
| 0.85 | 14.8 |
| 0.84 | 16.3 |
| 0.83 | 18.0 |
| 0.82 | 20.0 |
| 0.81 | 22.3 |
| 0.80 | 24.8 |
| 0.79 | 27.8 |
| 0.78 | 31.0 |
| 0.77 | 37.5 |

Table 3 Expanded values of $\alpha^2$, by the author

| $\alpha^2$ | $t$ hours |
|---|---|
| 1.00 | 1.0 |
| 0.99 | 1.1 |
| 0.98 | 1.3 |
| 0.97 | 1.5 |
| 0.96 | 1.7 |
| 0.95 | 2.0 |
| 0.94 | 2.3 |
| 0.93 | 2.7 |
| 0.92 | 3.1 |
| 0.91 | 3.6 |
| 0.90 | 4.1 |
| 0.89 | 4.6 |
| 0.88 | 5.1 |
| 0.87 | 5.6 |
| 0.86 | 6.2 |
| 0.85 | 6.7 |
| 0.84 | 7.2 |
| 0.83 | 7.8 |
| 0.82 | 8.3 |
| 0.81 | 8.9 |
| 0.80 | 9.4 |
| 0.79 | 10.0 |
| 0.78 | 10.6 |
| 0.77 | 11.1 |
| 0.76 | 11.7 |
| 0.75 | 12.2 |
| 0.74 | 13.3 |
| 0.73 | 14.0 |
| 0.72 | 15.0 |
| 0.71 | 15.9 |
| 0.70 | 16.9 |
| 0.69 | 17.8 |
| 0.68 | 19.9 |
| 0.67 | 20.0 |
| 0.66 | 21.0 |
| 0.65 | 22.5 |
| 0.64 | 23.8 |
| 0.63 | 26.0 |
| 0.62 | 28.0 |
| 0.61 | 31.0 |
| 0.60 | 34.9 |
| 0.59 | 42.0 |
| 0.60 | 34.9 |
| 0.59 | 42.0 |

Appendix 3 Value of $\theta'_{rm}$ as a function of $\lambda$ given by Equation 7

<table>
<tr><th>$q$</th><th>$m - n$</th><th>$|\bar{\zeta}_{wx}|$ $|\bar{\zeta}_{wy}|$</th><th>$\bar{\zeta}_{wx}$</th><th>$\bar{\zeta}_{wy}$</th><th>$\theta'_{rm}$ (degrees)</th></tr>
<tr><td rowspan="6">+</td><td rowspan="6">+</td><td rowspan="2">≤</td><td>+</td><td>+</td><td>$|\lambda|$</td></tr>
<tr><td>−</td><td>−</td><td rowspan="3">180 + $|\lambda|$</td></tr>
<tr><td rowspan="4">≥</td><td>−</td><td>−</td></tr>
<tr><td>−</td><td>+</td></tr>
<tr><td>+</td><td>+</td><td rowspan="2">$|\lambda|$</td></tr>
<tr><td>+</td><td>−</td></tr>
<tr><td rowspan="6">+</td><td rowspan="6">−</td><td rowspan="4">≤</td><td>+</td><td>+</td><td rowspan="2">90 − $|\lambda|$</td></tr>
<tr><td>−</td><td>+</td></tr>
<tr><td>−</td><td>−</td><td rowspan="3">270 − $|\lambda|$</td></tr>
<tr><td>+</td><td>−</td></tr>
<tr><td rowspan="2">≥</td><td>−</td><td>−</td></tr>
<tr><td>+</td><td>+</td><td>90 − $|\lambda|$</td></tr>
<tr><td rowspan="6">−</td><td rowspan="6">−</td><td rowspan="4">≤</td><td>+</td><td>+</td><td rowspan="2">90 + $|\lambda|$</td></tr>
<tr><td>−</td><td>+</td></tr>
<tr><td>−</td><td>−</td><td rowspan="3">270 + $|\lambda|$</td></tr>
<tr><td>+</td><td>−</td></tr>
<tr><td rowspan="2">≥</td><td>+</td><td>−</td></tr>
<tr><td>−</td><td>+</td><td>90 + $|\lambda|$</td></tr>
<tr><td rowspan="6">−</td><td rowspan="6">+</td><td rowspan="2">≤</td><td>−</td><td>+</td><td>180 − $|\lambda|$</td></tr>
<tr><td>+</td><td>−</td><td rowspan="3">360 − $|\lambda|$</td></tr>
<tr><td rowspan="4">≥</td><td>+</td><td>+</td></tr>
<tr><td>+</td><td>−</td></tr>
<tr><td>−</td><td>−</td><td rowspan="2">180 − $|\lambda|$</td></tr>
<tr><td>−</td><td>+</td></tr>
</table>

Although this table does not give all possible mathematical combinations of variables, it covers a sufficient range of combinations for all practical applications.

## Appendix 4 Definition of the highest surge and its indication.

The highest surge at a certain position in the North Sea is defined in this paper as the maximum value of surge height generated by a uniform wind field and its associated pressure field, over the sea, whose intensities are constant but directions are arbitrary.

The concept of this definition and a method of indicating the highest surge, in this paper, are illustrated below, although the actual computations are not carried out in this manner.

All the discussions in this paper, such as the effect of a pressure field on surge generation, should be applied only to the highest surge in this definition, e.g. a part shown by the thick line in each of (1) to (n), or the whole part of ($\Sigma$).

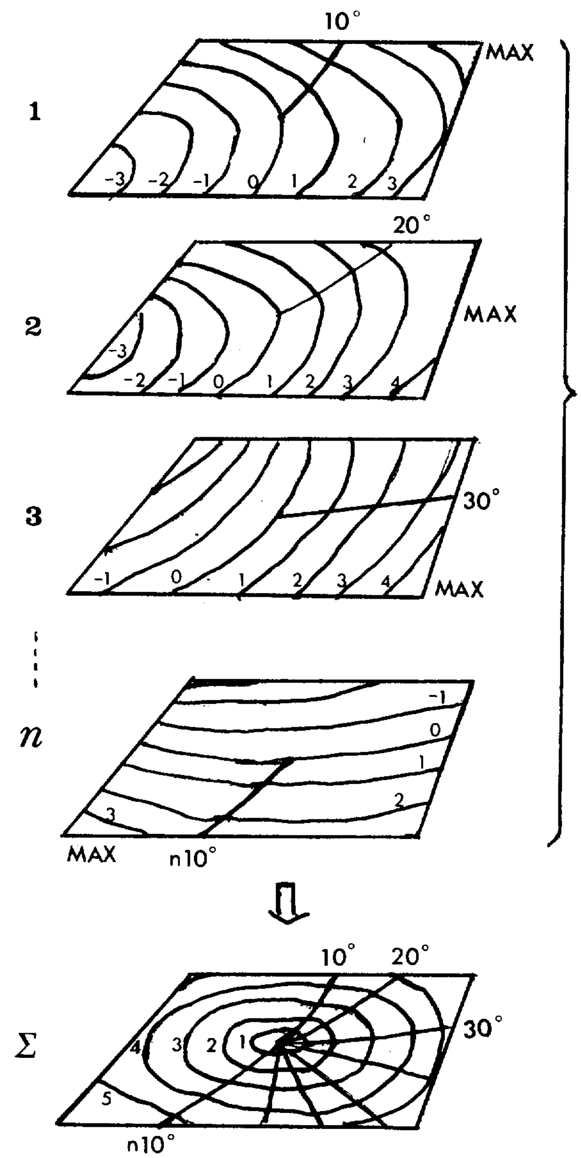


Contour maps of a surge in each wind direction.

Thick line crossing contours of each diagram shows the line along which highest surge throughout all the wind directions occurs.

The maximum surge throughout the sea area under each wind direction (shown by MAX) occurs in a certain part of the sea, but not necessarily the same part as the above mentioned line.

Synthesized diagram showing the highest surge at each position in the sea, and the direction of wind by which such a surge is generated.

Actual examples: Figs. 9, 11 and 12.